

RELATIVE EFFICIENCY COMPARISON OF CARBOXYMETHYL CELLULOSE (CMC) STABILIZED Fe^0 AND Fe^0/Ag NANOPARTICLES FOR RAPID DEGRADATION OF CHLORPYRIFOS IN AQUEOUS SOLUTIONS

A. V. BHASKAR REDDY^a, J. JAAFAR^{a*}, Z. ABDUL MAJID^a, A. ARIS^{b,c}, K. UMAR^{b,c}, J. TALIB^{b,c}, G. MADHAVI^d

^a*Department of Chemistry, Faculty of Science, Universiti Teknologi Malaysia, 81300 Johor Bahru, Johor, Malaysia*

^b*Centre for Environmental Sustainability and Water Security (IPASA), Research Institute for Sustainable Environment, Universiti Teknologi Malaysia, 81300 Johor Bahru, Johor, Malaysia*

^c*Department of Environmental Engineering, Faculty of Civil Engineering, Universiti Teknologi Malaysia, 81300 Johor Bahru, Johor, Malaysia*

^d*Department of Chemistry, Sri Venkateswara University, Tirupati, 517502, India*

This study investigated the rate of chlorpyrifos degradation with different carboxymethyl cellulose (CMC) stabilized and unstabilized iron-based nanoparticles viz. CMC- Fe^0 , CMC- Fe^0/Ag and Fe^0 under different concentrations of chlorpyrifos. FT-IR and SEM analysis indicated that CMC molecules were adsorbed to nanoparticles through the carboxylate (COO^-) and hydroxyl (OH^-) groups. All CMC stabilized nanoparticles exhibited excellent stability against aggregation because of both electrostatic and steric repulsions. The capability of CMC stabilized nanoparticles for the degradation of chlorpyrifos was investigated, which showed the maximum degradation with CMC- Fe^0/Ag and the least with Fe^0 nanoparticles when treated for about 4.0 hrs. The calculated first order rate constants (k_{obs}) were 0.377 hr^{-1} , 0.555 hr^{-1} and 0.749 hr^{-1} for Fe^0 , CMC- Fe^0 and CMC- Fe^0/Ag nanoparticles respectively. The rate of degradation increased as a function of Ag concentration in CMC- Fe^0/Ag nanoparticles. Temperature was also played an important role on the chlorpyrifos degradation, in which the rate constant of CMC- Fe^0/Ag nanoparticles declined from 0.910 hr^{-1} to 0.690 hr^{-1} when the temperature was altered from 35°C to 25°C . The stability experiments revealed that the CMC- Fe^0/Ag nanoparticles were stable and they were capable for the degradation of chlorpyrifos even after 3 months of their preparation.

(Received February 3, 2015; Accepted April 1, 2015)

Keywords: Carboxymethyl cellulose; Chlorpyrifos; Fe^0/Ag and Fe^0 nanoparticles; Reaction kinetics

1. Introduction

Chlorpyrifos is the fourth highest consuming organophosphorous insecticide extensively used throughout the world. It occupies about 38% of total pesticides used globally for agricultural control of wide range of insect species [1-3]. Like other organophosphorous pesticides, it inhibits acetyl cholinesterase, an essential enzyme for neuromuscular activities of either human or insects [4]. One of the most important problems associated with the use of chlorpyrifos is its persistence in the environment. Its continuous use has led to various disorders and diseases including cancer, adverse reproductive outcomes, peripheral neuropathies, neurobehavioral disorders and sensitization reactions, particularly of the skin [5,6]. Due to the environmental concerns associated with the accumulation of chlorpyrifos in soil and groundwater, there is a great need to develop safe, convenient and economically feasible methods for its degradation [7].

*Corresponding author: jafariah@kimia.fs.utm.my

Many physicochemical methods such as incineration, land filling, composting and chemical amendments have been used over the last few decades for the remediation of pesticide contaminated sites in the environment [8-11]. However, high cost and low efficiency limit their use in the remediation work [12, 13]. Remediation of pesticide contaminated sites using nano scale iron based materials is an emerging trend, providing opportunities to develop innovative site remediation technologies to solve environmental contamination problems of soil and water [14]. Infinitesimally small size (nm) and enhanced reactivity due to high surface area to volume ratio make iron nanoparticles as an excellent option for in-situ subsurface remediation. From the previous studies, it was found that the surface area of the nano iron was 1100 times greater than that of the microscale iron. Study has shown that 95% of trichloroethylene (TCE) dechlorination was observed by nano iron as compared to 86% by microscale iron [15]. The reported research supports that nano iron is an effective reductant in the treatment of chlorinated solvents [16, 17], nitro aromatic compounds [18-20], chlorinated pesticides such as dichlorodiphenyltrichloroethane (DDT), polychlorinated biphenyls, atrazine [21-23] and other organic compounds containing reducible functional groups [24, 25]. Recently, bimetallic particles (e.g. Pd/Fe, Ag/Fe) have been confirmed to exhibit high efficacy for the transformation of many chlorinated compounds and pesticides. Palladized iron for example, has been demonstrated to rapidly remove chlorinated ethenes such as PCB, PCE, TCE, c-DCE and t-DCE [26-29].

However, one drawback of nano iron particles is their tendency to form aggregates, thus making it difficult to prepare a stable suspension. Different stabilizers have been demonstrated to significantly inhibit aggregation and thus, increase the transportation of the nanoparticles. Starch has been reported to serve as a good dispersant for preparing nanoscale Ag particles in aqueous media [30]. Many biopolymers are available in nature, which could act as good dispersants to prevent the particle agglomeration as well as low cost and “greener” for environmental applications [31, 32].

The objective of the present study was to prepare different carboxymethyl cellulose (CMC) stabilized and unstabilized iron based nanoparticles viz. CMC- Fe^0 , CMC- Fe^0/Ag and Fe^0 in the laboratory using CMC as a stabilizer. During the synthesis, small amount (0.1% wt) of Ag was deposited on the surface of Fe^0 to prepare Fe^0/Ag bimetallic nanoparticles. Relative efficiency of Fe^0 , CMC- Fe^0 and CMC- Fe^0/Ag nanoparticles for the degradation of chlorpyrifos was investigated. Because of its large consumption, chlorpyrifos was chosen as the target compound. Chlorpyrifos degradation rate was evaluated with respect to the change of temperature and change of Ag concentration using CMC- Fe^0/Ag nanoparticles. Finally, the stability of CMC stabilized and unstabilized nanoparticles were also evaluated.

2. Materials and Methods

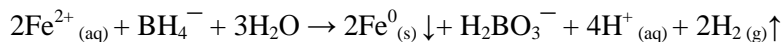
2.1 Reagents and standards

Chlorpyrifos (purity >99.9%) was purchased from Sigma-Aldrich (St.Louis, MO, USA). Fe (II) sulfate heptahydrate ($\text{FeSO}_4 \cdot 7\text{H}_2\text{O}$), sodium borohydride (NaBH_4), anhydrous sodium sulfate (Na_2SO_4) were obtained in their highest purity grade from Chem-Service (West Chester, USA). Carboxymethyl cellulose (CMC) was received from Texas Oil Corp (Mumbai, India). Ethanol, toluene, hexane, acetone and all other solvents used were of analytical grade. Silver nitrate (AgNO_3) was obtained from Fisher-Scientific (India) and the water used in this study was double distilled and deionized.

2.2 Preparation of nanoparticles

In the preparation of CMC- Fe^0 stabilized nanoparticles, $\text{FeSO}_4 \cdot 7\text{H}_2\text{O}$ stock solution was added to CMC solution to yield a solution with desired concentration. The solution was allowed to stand for 10 min to form complex with CMC. Here, the addition of CMC served as a dispersant and prevents the agglomeration of nanoparticles, thereby extending their reactivity. The Fe^{2+} concentration used in this study was 1.0 g/L and CMC concentration was 1.0% (w/w) of Fe^{2+} . In the next step, Fe^{2+} was reduced to Fe^0 using stoichiometric amount of sodium borohydride solution

at ambient temperature with vigorous stirring. NaBH₄ solids were dissolved in 0.1M NaOH because NaBH₄ was unstable in water and quickly result in a loss of reduction power. Addition of NaBH₄ to the FeSO₄ solution resulted in the rapid formation of fine black precipitate of CMC stabilized Fe⁰ according to the following reaction stoichiometry.



The evolution of H₂ gas ceased for 15 min and Fe⁰ nanoparticles were loaded with small amount of Ag by adding AgNO₃ to the CMC-Fe⁰ solution. The amount of Ag used in this study was 0.1% (w/w) of Fe. Because of the chainlike structure and macromolecular nature, CMC will not prevent the accessibility of CMC stabilized Fe⁰ particles for electron acceptors. Therefore, once Ag⁺ ions were added, they were reduced to Ag⁰ with the Fe nanoparticles and results in the formation of CMC-Fe⁰/Ag nanoparticles.

2.3 Characterization of CMC stabilized nanoparticles

Scanning electron microscope (SEM) analysis of all CMC stabilized and unstabilized nanoparticles were performed with CARL-ZEISS EVO MA 15 fitted with an Energy Dispersive X-ray Analysis (EDAX) System. The samples were observed at 10,000 x magnification with an accelerating voltage of 25 kV. FT-IR analyses of the samples were carried out in the mid-IR range using a Perkin-Elmer (USA) FT-IR Spectrum 2000 spectrometer. X-ray diffraction (XRD) analysis of CMC stabilized nanoparticles was performed using a SEIFERT 3003 TT X-ray Diffractometer. The analysis was performed at 40 kV and 40 mA with Cu-K α radiation at a wavelength of 1.542 Å. Brunauer-Emmett-Teller (BET) specific surface areas of nanoparticles was determined by N₂ gas adsorption using Micromeritics ASAP-2000 (USA). A Perkin-Elmer Model 3110 flame atomic absorption spectrophotometer (AAS) was used to obtain the quantitative recoveries of the metal ions in CMC-Fe⁰/Ag nanoparticles.

2.4 Batch experiment

Batch experiments were conducted to compare the efficiency of different CMC stabilized Fe⁰-based nanoparticles for the destruction of chlorpyrifos in aqueous solutions. Stock solution of chlorpyrifos was prepared by dissolving 0.1 g of chlorpyrifos in ethanol and further diluted with distilled water in the presence of small volume of ethanol to prevent turbidity. 50 mL of aqueous chlorpyrifos which gave initial concentration of 30 mg/L was mixed with 0.5 g (1.0%, w/v) of different Fe⁰-based nanoparticles in 100 mL Erlenmeyer flasks individually. The flasks were covered with parafilm M and agitated on a rotary shaker at 120 rpm at constant temperature of 28°C. Control experiments (without the addition of the nano particles) were carried out in parallel; all treatments were conducted in triplicate. The reaction times were recorded at the starting of mixing and the chemical analysis of the first duplicate sample at zero time was considered as the initial concentration of the reactant. At preselected time intervals, 2.0 mL aliquots were removed and transferred to polypropylene micro centrifuge tubes and centrifuged at 8000 x g for 10 min. Then, the chlorpyrifos aliquots were collected and extracted by adding equal volume (2.0 mL) of hexane and analyzed by using HPLC.

2.5 Chlorpyrifos analysis

Chlorpyrifos concentration in the samples were measured by reverse phase high performance liquid chromatography (RP-HPLC) using a Zorbax Rx C18 column (4.6 mm x 250 mm, 5.0 μm) with UV detector (at 230 nm). The analysis was performed using a mobile phase of acetonitrile-water (80:20, v/v) at a flow rate of 1.0 mL/min. Injection volume used was 20 μL and the retention time for chlorpyrifos was observed at 9.5 min.

3. Results and discussion

3.1 Characterization of Fe^0 , CMC- Fe^0 and CMC- Fe^0/Ag nanoparticles

Fig. 1 shows the representative SEM images of three different Fe^0 -based nanoparticles. It was observed that in the absence of CMC, the nanoparticles appeared as dendritic flocks rather than discrete particles; they were not well separated from each other and tend to form structures wherein large particles are capped with small particles. In the case of CMC- Fe^0 and CMC- Fe^0/Ag sample, nanoparticles appeared as much finer particles. The EDAX analysis of a single CMC- Fe^0/Ag nanoparticle sample indicated the presence of Fe and Ag as the major constituents. The FT-IR spectroscopy measurements were carried out to explore the modes of interactions between CMC and nanoparticle surface. The FT-IR spectra recorded for CMC and two Fe^0 -CMC stabilized nanoparticles is shown in Fig. 2. The peaks observed at strong absorbing bands corresponding to C–H bond stretching vibrations ($3300\text{--}2850\text{ cm}^{-1}$), O–H stretching vibrations (3600 cm^{-1}) and the weaker carbonyl/carboxyl stretching vibrations ($1740\text{--}1200\text{ cm}^{-1}$) show the transformation of the initial carboxylic acid ($\text{COOH} - 1690\text{ cm}^{-1}$) to a carboxylate ion ($\text{COO}^- - 1580\text{ cm}^{-1}$ and 1706 cm^{-1}) when bonding occurred to stabilize the nanoparticles. These data clearly indicate that there is no chemical interaction between the Fe^0 -based nanoparticles and CMC. The expected stabilization of nanoparticles was achieved probably due to electrostatic interactions between the two constituents, resulting into surface passivation. Such a property of the stabilizing agent could be highly desirable. BET surface area analysis gave the surface area of three different Fe^0 -based nanoparticles. The average particle diameter was determined to be in the range of 40–60 nm. Furthermore, the values are in good agreement with the sizes obtained by XRD data. In order to obtain the quantitative recovery of the metal ions in CMC- Fe^0/Ag nanoparticles, a Perkin-Elmer Model 3110 flame atomic absorption spectrometer was used and the results are presented in Table 1. From the data, we found that good recoveries were obtained for both Ag^+ and Fe^{2+} ions within the range of 95.8% and 98.4% with %RSD < 2.0.

Table 1. AAS recovery data of metal ions in CMC- Fe^0/Ag nanoparticles.

Metal ion	Added as	Concentration (mg/L)	Recovery (%)
Fe^{2+}	FeSO_4	1000	96.2 ± 0.84
Ag^+	AgNO_3	1.0	98.4 ± 1.93
		2.0	97.1 ± 1.24
		3.0	95.8 ± 1.85

%RSD calculated from 3 determinations

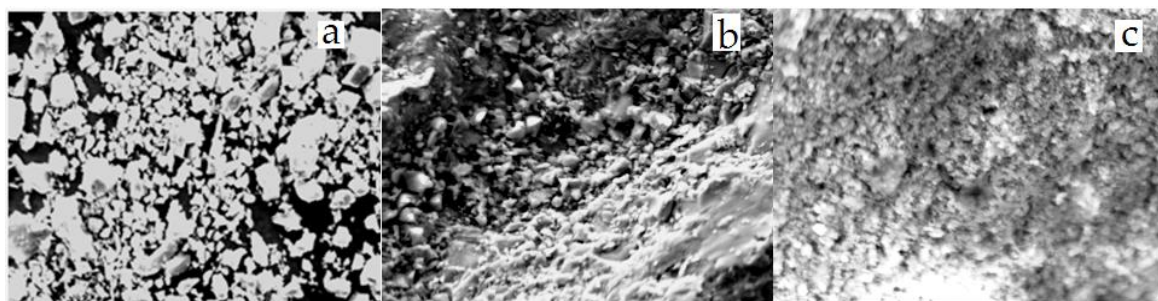


Fig. 1. SEM images of a) Fe^0 b) CMC- Fe^0 c) CMC- Fe^0/Ag nanoparticles.

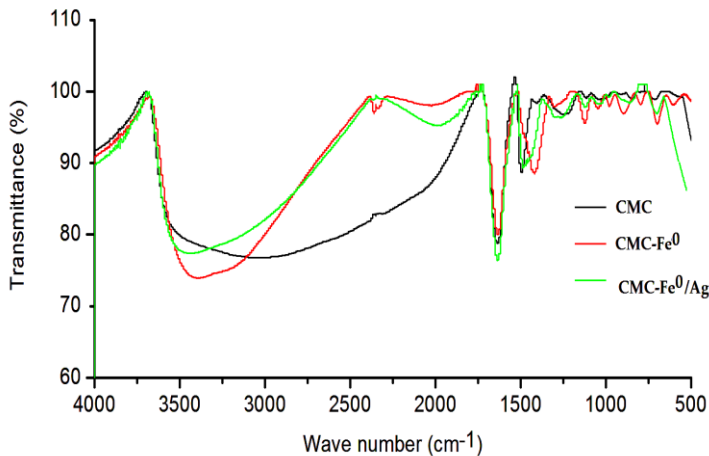


Fig. 2. FT-IR spectra of i) CMC ii) CMC- Fe^0 iii) CMC- Fe^0/Ag nanoparticles.

3.2 Chlorpyrifos degradation experiments

After treating the solution of chlorpyrifos (30 mg/L) with 1.0% (w/v) of three different types of nanoparticles, maximum chlorpyrifos degradation was achieved with CMC- Fe^0/Ag nanoparticles followed by CMC- Fe^0 nanoparticles after shaking for 4.0 hrs. Chlorpyrifos removal was least with unstabilized Fe^0 nanoparticles and no significant change was observed in the initial concentration of chlorpyrifos with blank experiments (without the addition of nanoparticles). Chlorpyrifos degradation was extremely high with CMC- Fe^0/Ag nanoparticles and the reaction roughly followed first order kinetics. The disappearance of chlorpyrifos with different nanoparticles over time is shown in Fig. 3. Up to 94% and 79% of chlorpyrifos was degraded with CMC- Fe^0/Ag and CMC- Fe^0 respectively, over the period of 4.0 hrs. Only 67% of chlorpyrifos was removed by the unstabilized Fe^0 nanoparticles. The corresponding rate constants were 0.377 hr^{-1} , 0.555 hr^{-1} and 0.749 hr^{-1} for Fe^0 , CMC- Fe^0 and CMC- Fe^0/Ag nanoparticles respectively. One possible reason for this is the presence of Ag (noble metal) as coating material, which gives an added dimension that allows electron transfer steps to proceed more rapidly and further progress towards stoichiometric use of the iron [33, 34]. In addition, CMC provided stability against particle agglomeration and Ag serves to facilitate the electron transfer step, because the rate of degradation is mainly influenced by electron transfer. The RP-HPLC chromatograms for chlorpyrifos degradation at different time intervals with CMC- Fe^0/Ag nanoparticles are shown in Fig. 4.

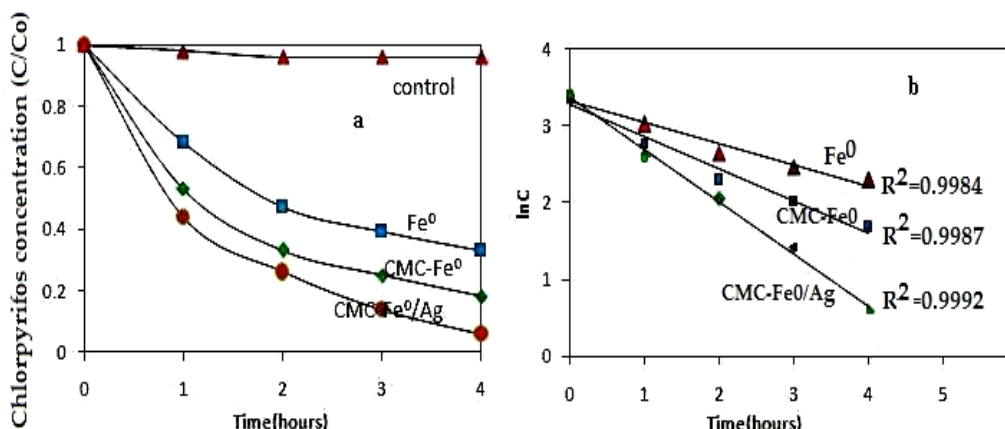


Fig. 3. a) Chlorpyrifos degradation using stabilized and unstabilized Fe^0 based nanoparticles at chlorpyrifos concentration of 30 mg/L b) First order kinetic model for chlorpyrifos degradation.

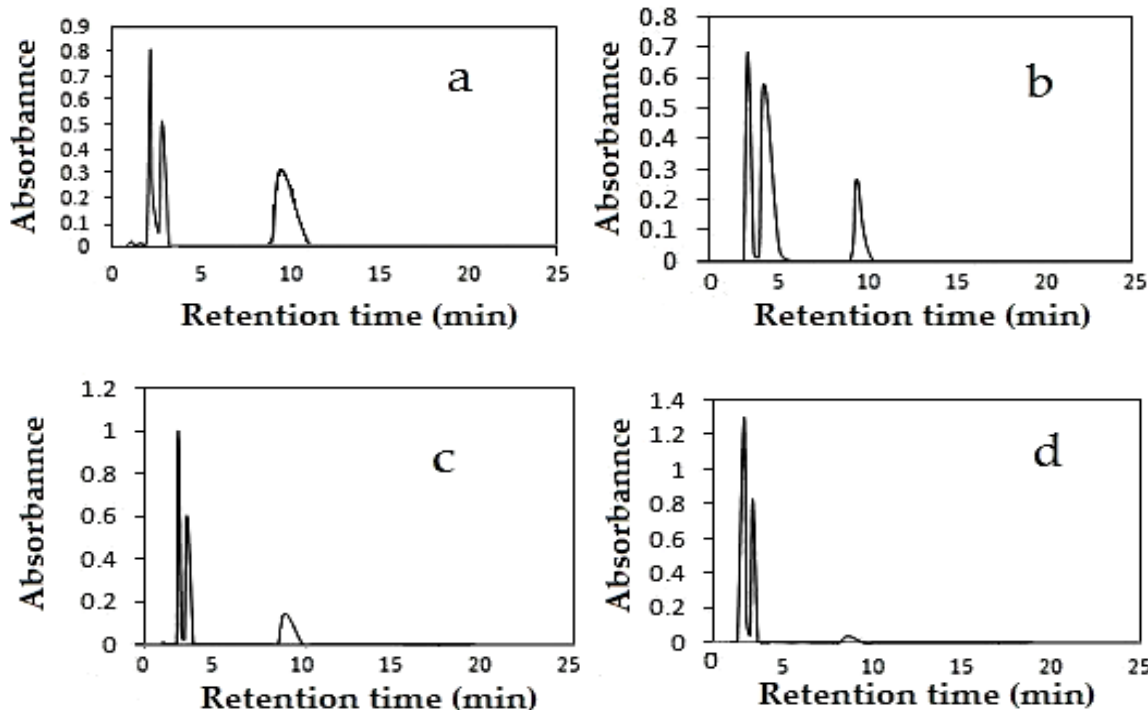


Fig. 4. HPLC chromatograms for chlorpyrifos degradation after treating with CMC- Fe^0/Ag nanoparticles at a) 1 hr b) 2 hrs c) 3 hrs and d) 4 hrs.

3.3 Effect of Ag concentration on degradation

The degradation rate of chlorpyrifos was measured as a function of Ag concentration in CMC- Fe^0/Ag nanoparticles and the results are represented in Fig. 5. As the concentration of Ag in CMC- Fe^0/Ag nanoparticles was increased, the reaction rate constants also increased. Therefore, the results indicated that the concentration of chlorpyrifos decreased exponentially in accordance with the Ag concentration, and the reaction was expected to follow pseudo-first order kinetics. Moreover, the degradation rate was improved when CMC was added to yield more dispersed iron nanoparticles. The following pseudo first-order reaction kinetics can be used to describe the chlorpyrifos degradation rate.

$$-\frac{dC}{dt} = k_{SA}a_sF_mC = k_{obs}C$$

where C is chlorpyrifos concentration (mg/L) at time t (hrs), k_{SA} is the specific reaction rate constant based on surface area of the nanoparticles ($\text{L}/\text{hr}/\text{m}^2$), a_s is the specific surface area of the nanoparticles (m^2/g), F_m is the mass concentration of the nanoparticles (g/L), and k_{obs} is the observed pseudo first order rate constant. The rate constants (k_{SA} or k_{obs}) were then determined by fitting the pseudo-first order rate expression from above equation to the experimental data. The values of k_{obs} were 0.713 hr^{-1} , 0.824 hr^{-1} , 1.16 hr^{-1} for 0.1% Ag, 0.2% Ag and 0.3% Ag with CMC- Fe^0/Ag nanoparticles, respectively. Surface area normalized rate constants are shown in Table 2. When the Ag content in CMC- Fe^0/Ag nanoparticles increased, the resulting particles diameter decreased. This increases the specific surface area of the resultant nanoparticles and therefore, enhances the surface reactivity of the nanoparticles per unit area [35].

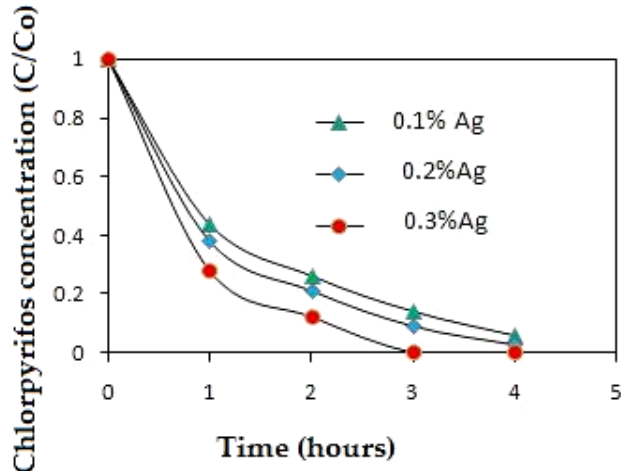


Fig. 5. Effect of Ag concentration on chlorpyrifos degradation with CMC-Fe⁰/Ag nanoparticles.

Table 2. Pseudo first-order rate constants of CMC-Fe⁰/Ag nanoparticles at different compositions.

Ag conc	k_{obs} (hr ⁻¹)	mean diameter (nm) CMC-Fe ⁰ /Ag	surface area (m ² /g)	k_{SA} (L/hr/m ²) calculated from BET
0.1%	0.713	28	27.2	2.62×10^{-3}
0.2%	0.824	18	42.3	1.94×10^{-3}
0.3%	1.166	12	63.5	1.82×10^{-3}

(Note: Mean diameter of different nanoparticles was calculated from XRD analysis.

Surface area calculated from $3 \times 10^6 / (r \times \rho)$, r = particle radius in nm ρ = density of Fe=7870kg/m³)

3.4 Effect of temperature on chlorpyrifos degradation

Degradation of chlorpyrifos with CMC-Fe⁰/Ag nanoparticles at different temperatures was also studied and the results are shown in Fig. 6 (a). According to the results, progressively better degradation of chlorpyrifos was observed at higher temperature i.e. 35°C. Only 92% of chlorpyrifos was removed in 4 hrs at 25°C, while the complete degradation of chlorpyrifos was observed within 3 hrs at a temperature of 35°C. The dependence of the reaction rates on temperature can be delineated with the Arrhenius equation. An interesting feature of the plot is the rate of degradation rapidly increased with increasing temperature. The degradation rate of chlorpyrifos fits well to the pseudo first-order kinetics. The rate constant for degradation of chlorpyrifos at 35°C was 0.910 hr⁻¹, which declined to 0.690 hr⁻¹ at 25°C. The change in the rate constant suggested that the temperature facilitated the degradation of chlorpyrifos in aqueous solutions. Applying the Arrhenius equation, the effect of temperature on degradation rates can be quantified using the following equation.

$$K = A \exp\left(-\frac{E_a}{RT}\right)$$

where K is rate constant, A is the frequency factor, Ea is the activation energy, R is ideal gas constant, and T is temperature. By plotting ln K versus 1/T, a linear least square analysis with good regression of 0.9987 is shown in Fig. 6 (b). The calculated activation energy for degradation of chlorpyrifos with CMC-Fe⁰/Ag was 0.189 kJ mol⁻¹, which is less than the activation energy of 16.6 kJ mol⁻¹ for hexachlorobenzene degradation with nZVI [22]. This indicates the good reactivity of CMC-Fe⁰/Ag nanoparticles and less temperature dependency for its application in degradation of environmental pollutants.

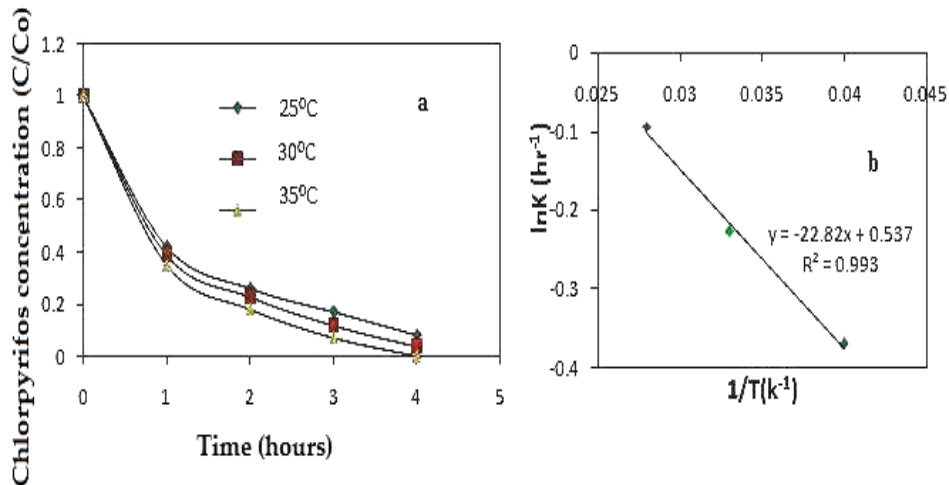


Fig. 6. a) Degradation kinetics of chlorpyrifos by CMC- Fe^0/Ag nanoparticles at different temperatures and b) Arrhenius plot of $\ln K$ vs $1/T$.

3.5 Stability of the synthesized nanoscale Fe^0 particles

The most frequently asked question regarding nanoparticle technology is the long-term performance and reactivity. Due to their small size and large surface area, the nanoparticles react very rapidly with a wide variety of oxidants in groundwater including dissolved oxygen, natural organic matter and water. To monitor the long-term performance of the different CMC stabilized Fe^0/Ag nano particles, experiments were conducted with all three Fe^0 -based nanoparticles after 3 months of their preparation. The degradation of chlorpyrifos with three different nanoparticles is plotted in Fig. 7. The observed chlorpyrifos degradation was 93%, 79% and 42% with CMC- Fe^0/Ag , CMC- Fe^0 and Fe^0 nanoparticles respectively. No considerable decrease in reactivity of CMC- Fe^0 and CMC- Fe^0/Ag nanoparticles was observed, which demonstrates the excellent reactivity up to 3 months in water slurries. However, a sharp decrease in reactivity of Fe^0 nanoparticles was observed, which is due to surface oxidation in very short time periods [29]. Freshly synthesized Fe^0 -based nanoparticles exhibit dark color. The observed color tends to change to light brown in a few hours and reddish-brown within few days, indicating extensive surface rusting or oxidation. However, a much slower color change was noticed for the CMC stabilized Fe^0 and Fe^0/Ag particles.

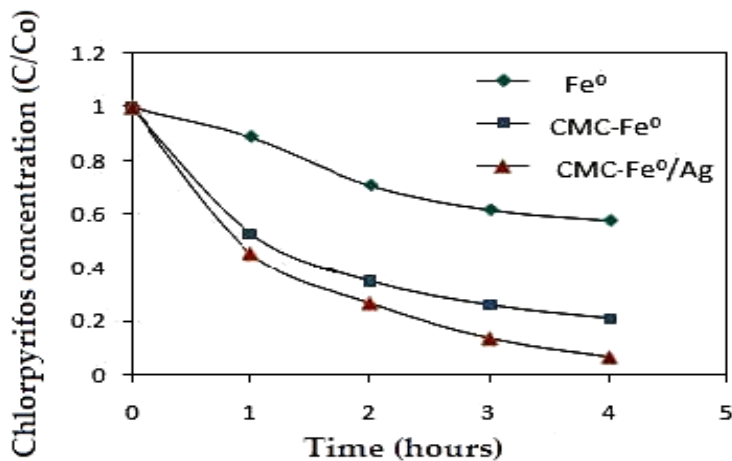


Fig. 7. Degradation study of chlorpyrifos with different nanoparticles after 90 days of their preparation.

4. Conclusions

The results of present study show that chlorpyrifos can be rapidly degraded by Fe⁰-based nano particles in aqueous solutions. The degradation of chlorpyrifos was found to be a pseudo first-order reaction. The reaction rate constants and degradation efficiency increased with the addition of Ag and CMC to Fe⁰ nanoparticles. Both the concentration of Ag and increase in temperature played a crucial role on the degradation of chlorpyrifos. The CMC-stabilized Fe⁰ and Fe⁰/Ag nanoparticles exhibited better removal efficiency and stability, because CMC acted as good dispersant and prevented the Fe⁰ nanoparticles from agglomeration. Results from the study suggest that CMC stabilized Fe⁰-based nanoparticles could be applicable for the on-site treatment of chlorpyrifos contaminated aqueous solutions.

Acknowledgements

The authors gratefully acknowledged the post doctoral financial support by the Research University Grant, Universiti Teknologi Malaysia and the Ministry of Education Malaysia for providing LRGS Grant on Water Security entitled Protection of Drinking Water: Source Abstraction and Treatment (203/PKT/6720006).

References

- [1] B. K. Singh, A. Walker, FEMS Micro. Rev. **30**, 428 (2006).
- [2] K. Stanek, D. Drobne, P. Trebse, Chemosphere, **64**, 1745 (2006).
- [3] T. Caceres, M. Megharaj,R. Naidu, Chemosphere, **66**, 1264 (2007).
- [4] P.K. Pradnya, B.J. Bhadbhade, N.M. Deshapande,S.S. Sarnaik, Ind. Nation. Sci. Acad. **70**, 57(2004).
- [5] T.H. Andersen, L. Wollenberger, T. Slothuus, R. Tjornhoj, A. Baun, Environ. Tox. Chem., **25**, 1187 (2006).
- [6] A. Murray, A.J. Rathbone,D.E. Ray, Environ.Toxicol.Pharmacol. **19**, 451(2005).
- [7] D.E. Salt, M. Blaylock, N.P.B.A. Kumar, V. Dushenkov, B.D. Ensley. I. Chet, I. Raskin, Bio-Tech. **13**, 468(1995).
- [8] A.V. Bhaskar Reddy, V. Madhavi, K. Gangadhara Reddy, G. Madhavi, Int. J. Res. Chem. Environ. **2**, 173(2012a).
- [9] E.S. Kempa, Int. J. Environ. Poll. **7**, 221(1997).
- [10] G. Wehtje, R.H. Walker, J.N. Shaw, Weed Sci. **48**, 248(2000).
- [11] B. Gunawardana, N. Singhal, P. Swedlund, Environ. Engineer. Res. **16**, 187(2011).
- [12] E. Dijkgraaf, H.R.J. Vollebergh, Ecolog. Econ. **50**, 233(2004).
- [13] J.J. Jin, Z.S. Wang, .H. Ran, Waste Management.**26**, 1045(2006).
- [14] T. Masciangioli, Z. Wei Xian, Environ. Sci. Tech. **37**, 102A(2003).
- [15] J. Cao, P. Clasen, W. Zhang, J. Mater. Res. **20**, 3238(2005).
- [16] R.A. Doong, Y.A. Lai, Chemosphere, **64**, 371(2006).
- [17] I. Hussain, Y.Q. Zhang, S.B. Huang, X.Z. Du. Chem. Engineer. J. **203**, 269(2012).
- [18] B.A. Till, L.J. Weathers, P.J.J. Alvarez, Environ. Sci .Tech. **32**, 634(1998).
- [19] Y.H. Huang, T.C. Zhang, P.J. Shea, S.D. Comfort, J. Environ. Qual. **32**, 1306(2003).
- [20] I. Sanchez, F. Stuber, J. Font, A. Fortuny, A. Fabregat, C. Bengoa, Chemosphere **68**, 338(2007).
- [21] M. Cao, L. Wang, W. Li, J. Chen, X. Lu, Chemosphere, **90**, 2303(2013).
- [22] D.G. Sayles, G. You, M. Wang, M.J. Kupferle, Environ. Sci. Tech. **31**, 3448(1997).
- [23] K. Geonha, J. Woohyeok, C. Seunghee, J. Hazard. Mater. **155**, 502(2008).
- [24] Y.P. Sun, X. Li, J. Cao,W. Zhang, H.P. Wang, J. Coll. Inter. Sci. **120**, 47(2006).
- [25] B. Lai, H. Hong Zhang, R. Li, Y.X. Zhou, J. Wang, Chem. Engineer. J. **249**, 143(2014).

- [26] C. Grittini, M. Malcomson, Q. Fernando, N. Korte, Environ. Sci. Tech. **29**, 2898(1995).
- [27] R. Muftikian, Q. Fernando, N. Korte, Wat. Res. **29**, 2434(1995).
- [28] X.Y. Wang, C. Chen, Y. Chang, H.L. Liu, J. Hazar. Mat. **161**, 815(2009).
- [29] N. Sakulchaicharoen, D.M. O'Carroll, J.E. Herrera, J. Contamin. Hydro. **118**, 117(2010).
- [30] F. He, D. Zhao, Environ. Sci. Tech. **39**, 3314(2005).
- [31] A.V. Bhaskar Reddy, V. Madhavi, K. Gangadhara Reddy, G. Madhavi, J. Chem, Article ID 521045, 1(2013).
- [32] A.V. Bhaskar Reddy, K. Gangadhara Reddy, V. Madhavi, G. Madhavi, Int. J. Sci. Innov. Discov. **2**, 106(2012b).
- [33] X.H. Xu, H.Y. Zhou, P. He, D.H. Wang, Chemosphere, **58**, 1135 (2008).
- [34] S. Luo, S. Yang, X. Wang, C. Sun, Chemosphere, **79**, 672 (2010).
- [35] L.M. Liz Marzan, A.P. Philipse, J. Phy. Chem. **99**, 15120 (1995).